

Self-ordering in diffusion-controlled reactions: Exciton fusion experiments and simulations on naphthalene powder, percolation clusters, and impregnated porous silica

S. J. Parus and R. Kopelman

Department of Chemistry, University of Michigan, Ann Arbor, Michigan 48109

(Received 13 September 1988)

Reactive self-ordering is demonstrated for the elementary reaction $A + A \rightarrow \text{product}$ in low-dimensional media, via both simulations and experiments. In one dimension, an effective spacing of excitations is created (order of 10 lattice units). The experimental verification involves excitation-time modulation, a new technique for microstructural studies. Naphthalene-impregnated porous glass (Vycor), naphthalene isotopic alloys, and naphthalene crystalline powder all show the self-ordering effect for triplet exciton annihilation.

INTRODUCTION

Macroscopic self-ordering or self-segregation in elementary, diffusion-limited reactions has been predicted for the $A + B \rightarrow 0$ reaction from both theory and simulations.¹ However, to the best of our knowledge, such ordering has never been verified experimentally. This is not surprising because the models used were based on mathematical constraints that are experimentally unrealistic, such as a strict equality of A and B particles coupled with a random generation process.¹ On the other hand, for the simpler reactions, $A + A \rightarrow \text{product}$, self-ordering occurs naturally (but obviously not segregation). Indeed, self-ordering for the $A + A \rightarrow 0$ and $A + A \rightarrow A$ reactions has been implicit in recent theoretical work,²⁻¹² but no explicit criterion and no spatial distributions have been given.¹³ Here we provide criteria and show the self-ordering explicitly, via Monte Carlo simulations. Furthermore, we demonstrate a self-ordering in exciton fusion experiments. In contrast to the macroscopic segregation predicted for $A + B$ reactions, one finds a mesoscopic ordering, with gratinglike structures, for the $A + A$ reactions at low dimensions.

The explicit nature of the ordering is simulated here for the one-dimensional case, based on the closest-neighbor distance as a new order criterion. This ordering accounts for the nonclassical, steady-state²⁻⁸ and transient,⁹⁻¹⁹ reaction kinetics and exciton fusion kinetics demonstrated earlier for low-dimensional ($d \leq 2$) media. It also makes possible a simple, but powerful, new experimental technique for the characterization of low-dimensional or disordered media.^{7,8} Most important, we present what we believe to be the first direct experimental verification of the reactive self-ordering of excitons.

SIMULATIONS

The experimental exciton reaction; triplet + triplet \rightarrow triplet or singlet, where singlet \rightarrow triplet or fluorescence, was simulated by reactive random walkers ($A + A \rightarrow 0$ and $A + A \rightarrow A$) on a variety of lattices. Comparisons were made between different initial conditions. Steady-state conditions were generated by adding several new

walkers per step until the total number of walkers was constant. Pulsed conditions were then studied by adding, in one step, the same number of walkers that exist at steady state to produce an initial uniformly random distribution. In both cases, after stopping the addition of walkers ($t = 0$), the number of walkers or reactants remaining at time t (monitored experimentally by phosphorescence) and the number of annihilations or reaction rate at time t (monitored experimentally by delayed fluorescence) were monitored on the computer. While the initial ($t = 0$) global densities are equal for both forms of reactant generation, this does not guarantee equal reaction rates at $t \geq 0$ or equal global densities at $t > 0$. Examples are given in Fig. 1 which is discussed further below.

The spatial and temporal aspects of a distribution of reacting particles (excitons) are related. The simulations show this most clearly for a one-dimensional lattice. Fig-

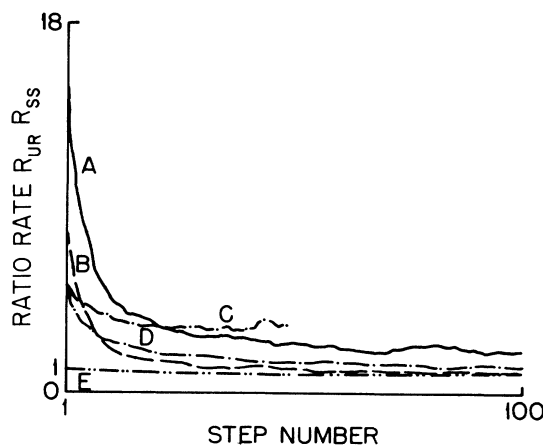


FIG. 1. Simulation examples of time-modulation technique. Ratio of annihilation reaction rates R_{ur}/R_{ss} (uniformly random pulse over steady-state generated population) vs step number, for the simulation $A + A = 0$ on various lattices (total number of sites = 30 000). Curve A, one-dimensional islands (20 sites each); curve B, one-dimensional continuous chain; curve C, three-dimensional islands ($3 \times 3 \times 3$ sites each); curve D, three-dimensional percolation clusters (cubic; 40% occupation, all clusters); curve E, three-dimensional cube.

ure 2 gives the distribution of interparticle (closest neighbor) gaps in terms of gap lengths. This is equivalent to the Hertz nearest-neighbor continuum distributions.²⁰ For a Poissonian (uniformly random) distribution of particles, the most probable gap is the shortest one ($l=1$ lattice unit), giving a quasiexponential Hertz-like distribution of gaps. This is no longer true for the steady-state distribution. Here, there is a most probable gap length ($l > 1$) with a curve resembling a skewed exponential or skewed Gaussian (Wigner-like) distribution.^{21,22} (Such a distribution would also be generated by a sinusoidal position distribution, e.g., an exciton population created by a weak transient grating.) We note that the random distribution represents a spatially uniform, pulse-created exciton distribution. Allowing each one of the two realizations (pulsed and steady state) to relax reactively (with no further supply of particles), one finds two different reactive decay curves in spite of the equality of populations for both realizations. The *initial* decay rate will differ most drastically as it is only determined by reactant pairs with a gap $l=1$. There are many more such $l=1$ gaps for the pulsed distribution than for the steady-state distribution, the ratio being about ten for the one-dimensional lattice (see Fig. 2). Figure 1 (curve B) plots the ratio of reaction (fusion) probability as a function of time for the one-dimensional lattice. At $t=0$, this ratio is about eight. The two ratios (of pair formation and of reactivity) are related (but not equal). In principle, curve B of Fig. 1 carries the information given in Fig. 2. It is obvious from Fig. 1 that the most significant steady-state ordering occurs for one-dimensional islands (filaments). On the other hand, there is no ordering effect for a cubic lattice. Other topologies show an intermediate behavior (which is highly specific). The simulations of Fig. 1 give the temporal aspect, which is closest to our experiments. We em-

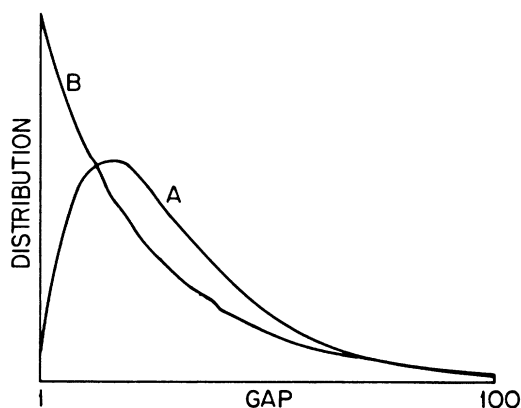


FIG. 2. Simulation examples of self-ordered and random populations. Relative distribution of the interparticle closest-neighbor distance ("gap") l , in number of lattice units for each particle, on a one-dimensional lattice with 30 000 sites. Curve A, reactive steady state ($A+A \rightarrow 0$, density = 2%), after 2000 steps of adding two particles per step, averaged over 1000 realizations; curve B, uniformly random distribution of the same number of particles as in curve A with no reaction steps taken. Note that for the gap length $l=1$, the gap population (0.0404 of total) is 10.7 times that of curve A.

phasize here that, for each topology, the initial populations (steady-state and pulsed) are strictly equal. This is also the key for the design of meaningful experiments (see below).

The "pulsed" (random) curve of Fig. 2 fits the one-dimensional Hertz-like distribution²⁰ $P(l)$ of nearest-neighbor lattice distances l ,

$$P(l) = 2c \exp(-2cr), \quad r = l - 1, \quad (1)$$

where c is the concentration of particles on the lattice. However, the kinetic steady-state curve of Fig. 2 ($A+A \rightarrow 0$) fits the skewed exponential distribution $K(l)$:

$$K(l) = Al \exp(-Br), \quad (2)$$

where $A \sim c^2$ and $B \sim c$, as required by dimensional analysis. Furthermore, for the transient ("big bang") reaction $A+A \rightarrow A$, we find an excellent fit with a skewed Gaussian (Wigner-like) distribution

$$K'(l) = A'l \exp(-B'r^2), \quad (3)$$

where $A' \sim c^2$ and $B' \sim c^2$, for long times (more than 1000 time steps). For a given reaction the steady-state and transient reactions exhibit similar but not the same kinetic distributions, i.e., Eq. (2) for transient $A+A \rightarrow 0$ and Eq. (3) for steady-state $A+A \rightarrow A$ have to be appropriately modified. Finally, we note that, based on the simple argument that the global reaction rate (R) is given by²³⁻²⁵ $R \sim cK(l \rightarrow 1)$ one recovers the rigorous^{2,3} reaction law, which applies to both the steady-state and the transient ($t \rightarrow \infty$) cases, i.e., $R \sim c^3$, for both $A+A \rightarrow 0$ and $A+A \rightarrow A$ reactions.

EXPERIMENTS: TIME MODULATION TECHNIQUE

Triplet fusion experiments were performed on naphthalene-impregnated porous glass (Vycor), naphthalene powder and perfectly crystalline isotopic alloys of naphthalene ($C_{10}H_8:C_{10}D_8$). These samples cover a dimensionality range between one and three for exciton transport.^{6,26} Purification, preparation, and other experimental procedures were the same as in previous studies.^{23,26-28} We only describe here the details pertaining to the new ("time modulation") technique. The time dependence of the naphthalene triplet-triplet exciton annihilation reaction rate was monitored, as usual, via the delayed fluorescence emission. Phosphorescence emission corresponds to the instantaneous triplet reactant concentration (global density). The dependence of the relative decay rates and intensities of the emissions on *initial excitation duration* was examined. "Time modulation" pertains to the modulation of this excitation duration. A random population of excitons was produced by pulsed excitation (e.g., 5 msec duration) from a mechanically shuttered xenon arc lamp. The steady-state population was created by leaving the shutter open for several seconds (which is longer than the time required to establish a constant phosphorescence signal). Neutral-density filters were used to give a phosphorescence intensity at time zero (the closing time of the shutter) equal to that obtained from the pulsed excitation. This insures equal initial global exciton densities. However, this equalization is not

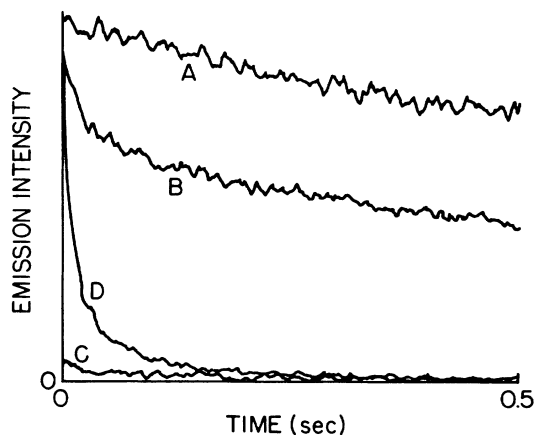


FIG. 3. Relative intensities of phosphorescence and of delayed fluorescence decays from naphthalene in porous Vycor glass at 18 K following steady-state (11 sec duration) or pulsed (20 msec duration) excitation (319 nm). Curve A, phosphorescence from steady-state excitation with a number 2.0 neutral density filter to equalize its initial intensity to that of curve B; curve B, phosphorescence from pulsed excitation; curve C, delayed fluorescence from conditions in curve A; curve D, delayed fluorescence from conditions in curve B. Note that the intensity scale for curves C and D is different than that for curves A and B.

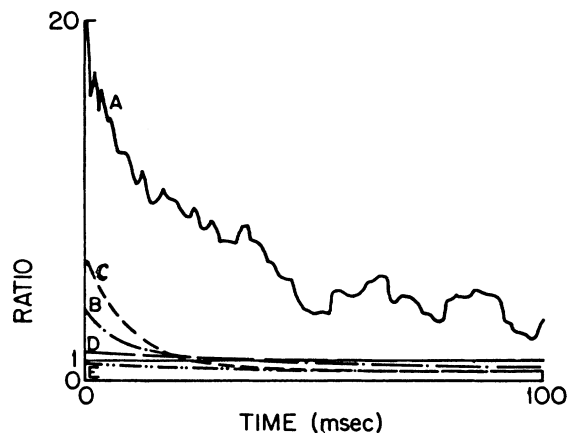


FIG. 4. Ratio of delayed fluorescences: pulsed vs steady-state excitation, with equalized initial phosphorescence intensities. Curve A, naphthalene in porous Vycor glass; curve B, naphthalene powder; curve C, 5% isotopic mixed naphthalene crystal; curve D, 11% isotopic mixed crystal; curve E, 39% isotopic mixed crystal. Note that the deviations from the classical value (unity) are up to 2000% and exceed by far the "noise."

sufficient to assure equal initial annihilation kinetics. Both the phosphorescence and the delayed fluorescence time decays are quite different for the pulsed and steady-state cases. Figure 3 shows the results for naphthalene-impregnated porous glass. Similar results are obtained for naphthalene powder and for low-concentration naphthalene single-crystal isotopic alloys ($C_{10}H_8$ below percolation^{6,14-16}). These samples also exhibited low-dimensional exciton transport in other studies.^{6,26} On the other hand, no such differences in intensities or decay rates are observed for high-concentration alloys (above percolation) or for nearly perfect naphthalene crystals. Above percolation, the single-crystal alloy exhibits classical rather than geometrically restricted transport characteristics⁶ and no self-ordering is expected. This range of behaviors is shown in Fig. 4. (These well-studied percolation systems^{6,14-16} were chosen to test the validity of the time modulation method.)

We can relate the measured temporal features to the microscopic spatial features with the aid of the simulations. For instance, from Figs. 1 and 4 it appears that the porous Vycor naphthalene filaments have an effectively one-dimensional, wormlike topology. Our computer modeling implies that the naphthalene "plugs" have the shape of one-dimensional islands, i.e., filaments whose length is an order of magnitude above their width. The filament width is limited by the pore "diameter" (4-6 nm) but could be as low as 2 nm. This suggests a filament length

of 20-100 nm. Similar conclusions^{23,26-28} were obtained from long-time decays of phosphorescence and delayed fluorescence.²⁹ Specifically, it is evident from Figs. 4 and 1 that a percolation network of pores is not likely to be consistent with our naphthalene in Vycor results.^{30,31} However, a complete study of the Vycor and powder results is reserved for a later work.

SUMMARY

Our experiments demonstrate a nonrandom distribution, i.e., kinetic self-ordering, for the triplet exciton populations in naphthalene samples that are *not* pure and perfect bulk crystals: crystalline powders, naphthalene filaments in porous silica, and isotopic alloys with compositions below percolation. However, for isotopic alloys with compositions well above percolation, the exciton distribution is random within our experimental accuracy. A new method for studying topology and disorder, the excitation-time-modulation method, has thus been introduced. The simulation results are consistent with the experimental effects. Furthermore, for one-dimensional topologies they show non-Hertzian, skewed exponential or Wigner-like steady-state reactant distributions, implying the existence of organized, gratinglike steady-state exciton distributions, i.e., a self-ordering of excitations on a mesoscopic distance scale.

This work was supported by National Science Foundation Grant No. DMR-8303919.

- ¹A. A. Ovchinnikov and Ya. B. Zeldovich, *Chem. Phys.* **28**, 215 (1978), and references therein; D. Toussaint and F. Wilczek, *J. Chem. Phys.* **78**, 6242 (1983); A. Blumen, J. Klafter and G. Zumofen, in *Optical Spectroscopy of Glasses*, edited by I. Zschokke (Reidel, Dordrecht, 1986), p. 51; K. Kang and S. Redner, *Phys. Rev. Lett.* **52**, 955 (1984); P. Meakin and H. E. Stanley, *J. Phys. A* **17**, L173 (1984); Z. Yi-Cheng, *Phys. Rev. Lett.* **59**, 1726 (1987); **60**, 1885 (1988); K. Lindenberg, B. J. West, and R. Kopelman, *ibid.* **60**, 1777 (1988); D. ben Avraham and C. Doering, *Phys. Rev. A* **37**, 5007 (1988); S. Kanno, *Prog. Theor. Phys.* **79**, 721 (1988); L. W. Anacker and R. Kopelman, *Phys. Rev. Lett.* **58**, 289 (1987); L. W. Anacker and R. Kopelman, *J. Phys. Chem.* **91**, 5555 (1987).
- ²Z. Racz, *Phys. Rev. Lett.* **55**, 1707 (1985); J. L. Spouge, *Phys. Rev. Lett.* **60**, 871 (1988); **60**, 1885 (1988).
- ³L. W. Anacker and R. Kopelman, *J. Chem. Phys.* **81**, 6402 (1984).
- ⁴J. S. Newhouse and R. Kopelman, *Phys. Rev. B* **31**, 1677 (1985).
- ⁵J. S. Newhouse and R. Kopelman, *J. Chem. Phys.* **85**, 6804 (1986).
- ⁶R. Kopelman, *J. Stat. Phys.* **42**, 185 (1986).
- ⁷R. Kopelman and S. J. Parus, in *Fractal Aspects of Materials II*, edited by D. W. Schaefer, R. B. Laibowitz, B. B. Mandelbrot, and S. H. Liu (Materials Research Society, Boston, 1986), Vol. EA-10, p. 50.
- ⁸R. Kopelman, in *Fractal Aspects of Materials; Disordered Systems*, edited by A. J. Hurd, D. A. Weitz, and B. B. Mandelbrot (Materials Research Society, Boston, 1987), Vol. EA-13, p. 112.
- ⁹D. C. Torney and H. M. McConnel, *J. Phys. Chem.* **87**, 1441 (1983).
- ¹⁰P. V. Elyutin, *J. Phys. C* **17**, 1867 (1987).
- ¹¹P. Evesque and J. Duran, *J. Chem. Phys.* **80**, 3016 (1984).
- ¹²G. Zumofen, A. Blumen, and J. Klafter, *J. Chem. Phys.* **82**, 3198 (1985).
- ¹³However, a new theoretical paper appeared after the submission of this one: C. R. Doering and D. ben-Avraham, *Phys. Rev. A* **38**, 3035 (1988) based on an older mathematical paper: M. Bramson and D. Griffeath, *Ann. Probab.* **8**, 183 (1980), which also obtained the "Wigner-like" distribution for the transient $A+A \rightarrow A$ reaction in one dimension and additionally considered the $A+A \rightarrow 0$ reaction. The mesoscopic self-ordering is noted and related simulations are given by Doering and ben-Avraham. Such simulations and observations were also made earlier by the present authors (see Refs. 7 and 8) and are given in two review articles: R. Kopelman, *Science* **241**, 1620 (1988); R. Kopelman, S. J. Parus, and J. Prasad, *Chem. Phys.* (to be published).
- ¹⁴R. Kopelman, J. Hoshen, J. S. Newhouse, and P. Argyrakis, *J. Stat. Phys.* **30**, 355 (1983).
- ¹⁵P. W. Klymko and R. Kopelman, *J. Lumin.* **24/25**, 457 (1981); P. W. Klymko and R. Kopelman, *J. Phys. Chem.* **86**, 3686 (1982).
- ¹⁶P. W. Klymko and R. Kopelman, *J. Phys. Chem.* **87**, 4565 (1983).
- ¹⁷P. Argyrakis and R. Kopelman, *J. Phys. Chem.* **91**, 2699 (1987).
- ¹⁸L. W. Anacker, R. P. Parson, and R. Kopelman, *J. Phys. Chem.* **89**, 4758 (1985).
- ¹⁹L. Li and R. Kopelman, *J. Lumin.* **40/41**, 688 (1988).
- ²⁰P. Hertz, *Math. Ann.* **67**, 387 (1909); S. Chandrasekhar, *Rev. Mod. Phys.* **15**, 1 (1943); E. W. Montrol and W. W. Badger, *Introduction to Quantitative Aspects of Social Phenomena* (Gordon and Breach, New York, 1974), p. 100.
- ²¹D. Delande and J. C. Gay, *Phys. Rev. Lett.* **57**, 2006 (1986); **57**, 2877 (1986).
- ²²M. L. Mehta, *Random Matrices and the Statistical Theory of Energy Levels* (Academic, New York, 1967).
- ²³R. Kopelman, S. J. Parus, and J. Prasad, *Chem. Phys.* (to be published); R. Kopelman, *Science* **241**, 1620 (1988).
- ²⁴E. Clement and R. Kopelman (unpublished).
- ²⁵L. Li, E. Clement, P. Argyrakis, L. A. Harmon, S. J. Parus, and R. Kopelman, *Fractal Aspects of Materials; Disordered Systems II* (Materials Research Society, Boston, in press); G. Weiss, R. Kopelman, and S. Havlin, *Phys. Rev. A* **39**, 466 (1988).
- ²⁶R. Kopelman, S. Parus, and J. Prasad, *Phys. Rev. Lett.* **56**, 1742 (1986).
- ²⁷J. Prasad and R. Kopelman, *Phys. Rev. Lett.* **59**, 2103 (1987).
- ²⁸R. Kopelman, L. Li, S. J. Parus, and J. Prasad, *J. Lumin.* **38**, 289 (1987).
- ²⁹The previous long-time technique is based on the anomalous diffusion (compact random walk) in low dimensions while the current short-time technique is based on the anomalous distributions of the reactive populations at low dimensions. Obviously, there is a direct relation between the compactness of the diffusion and the ordering of the reactants. However, the long-time decay experiments are weighted more heavily by reactions on longer naphthalene filaments (worms) while the current short-time decays may be weighted more heavily by reactions on shorter filaments. We thus estimate a filament length of about 200–1000 Å or longer, with an effective one-dimensional topology. Thus, even though the naphthalene plugs do not entirely fill the pores, this still implies a Vycor pore topology that is quasi-one-dimensional over a range of 200 Å and possibly 1000 Å or longer. Such a picture is consistent with some literature conclusions [see D. W. Schaefer, B. C. Bunker, and J. P. Wilcoxon, *Phys. Rev. Lett.* **58**, 284 (1987)] but not with others [U. Even, K. Rademann, J. Jortner, N. Manor, and R. Reisfeld, *Phys. Rev. Lett.* **58**, 285 (1987); **52**, 2164 (1984)].
- ³⁰On a very short time scale (several exciton hops) the naphthalene filaments may appear to be three dimensional. However, within our time resolution (20 ms), even the pulse-created excitons will have explored the entire filament radius. The steady-state created exciton distribution has obviously ample time to sample the one-dimensional topology.
- ³¹W. D. Dozier, J. M. Drake, and J. Klafter, *Phys. Rev. Lett.* **56**, 197 (1986).